Keldysh Institute • Publication search

Keldysh Institute preprints • Preprint No. 47, 2015

Ivanov D.S., Ovchinnikov M.Yu.,
Penkov V.I., Roldugin D.S.,
Doronin D.M., Ovchinnikov A.V.

Three-axis satellite stabilization using only magnetorquers and magnetometer

Recommended form of bibliographic references: Ivanov D.S., Ovchinnikov M.Yu., Penkov V.I., Roldugin D.S., Doronin D.M., Ovchinnikov A.V. Three-axis satellite stabilization using only magnetorquers and magnetometer // Keldysh Institute Preprints. 2015. No. 47. 20 p. URL: http://library.keldysh.ru/preprint.asp?id=2015-47&lg=e

О р д е н а Л е н и н а
ИНСТИТУТ ПРИКЛАДНОЙ МАТЕМАТИКИ
имени М.В. Келдыша
Р о с с и й с к о й а к а д е м и и н а у к

D.S. Ivanov, M.Yu. Ovchinnikov, V.I. Penkov,
D.S. Roldugin, D.M. Doronin, A.V. Ovchinnikov

Three-axis satellite stabilization using only magnetorquers and magnetometer

Moscow — 2015

Иванов Д.С., Овчинников М.Ю., Пеньков В.И., Ролдугин Д.С., Доронин Д.М., Овчинников А.В.

Использование магнитных катушек и магнитометра для обеспечения трехосной ориентации спутника

Рассматривается спутник, оснащенный магнитной системой ориентации в составе трех взаимно перпендикулярных магнитных катушек и трехкомпонентного магнитометра. Спутник стабилизируется в орбитальной системе координат в неустойчивом в гравитационном поле положении равновесия. Рассматриваются два подхода к реализации управления. Показана возможность обеспечения трехосной ориентации спутника с использованием минимального состава аппаратных средств. Исследуется влияние ошибок в знании моментов инерции аппарата и возмущающих моментов на точность ориентации.

Ключевые слова: магнитная система ориентации, магнитометр, трехосная ориентация, фильтр Калмана

Danil Ivanov, Mikhail Ovchinnikov, Vladimir Penkov, Dmitry Roldugin, Dmitry Doronin, Andrey Ovchinnikov

Three-axis satellite stabilization using only magnetorquers and magnetometer

Attitude motion of a satellite equipped with magnetic control system is considered. System comprises of three mutually orthogonal magnetorquers and one three-axis magnetometer. Satellite is stabilized in orbital reference frame in equilibrium position unstable in gravitational field. Two control strategies are presented. Three-axis attitude is shown to be achievable. Accuracy in presence of disturbing torques and inertia moments uncertainty is assessed.

Key words: magnetic attitude control system, three-axis magnetometer, three-axis attitude, Kalman filter

The work was supported by RFBR grant 15-31-20058.

Contents

Introduction

Magnetic control systems are widely used for satellite attitude stabilization. The main intrinsic problem with magnetic control is underactuation. Control torque direction is always restricted to the plane perpendicular to the local magnetic field vector. Magnetic three-axis control is discussed in this paper following results obtained in [1,2]. These previous works support the possibility of such a control and provide recipes for proper control parameters adjustment. This paper focuses on numerical simulation of satellite attitude under soft assumptions relevant to real orbital motion. The most important feature relates to the attitude determination problem. This process is modelled also. Furthermore attitude sensors are restricted to a three-axis magnetometer. It is impossible to reconstruct three-axis attitude using one vector measurement. However geomagnetic induction vector rotation allows Kalman filter implementation. Vector motion is included in filter mathematical model for the system and sensor readings. The similar system with magnetic torquers and magnetometer is considered in [3] for achieving three-axis attitude stabilization, but control algorithm is based on SDRE (state-dependant Riccati equation) technique.

The problem of attitude determination with magnetometer measurements is well studied. Psiaki et.al. were among the first who proposed application of the extended Kalman filter for this problem [4]. Besides quaternion vector part and angular velocity vector authors estimate disturbing torque acting on gravitationally stabilized satellite. The -paper considers influence of models parameters on the estimation accuracy. Self-initializing filter guaranteeing convergence with any initial state vector estimate is proposed in [5,6]. Special modification of the algorithm is developed in [7] for a fast-rotating satellite. Interesting two-step Kalman filter is applied for attitude motion determination in [8]. Magnetic field derivative is determined first. It is then used for state vector estimation. Orbital motion may be estimated along with angular [9,10]. This requires significant computational effort and may not be applicable for microsatellites on-board computers. Present paper focuses on the application of the extended Kalman filter with minimal state vector for satellite stabilized by magnetic torquers only. Approach proposed by the authors in [11] is used for Kalman filter tuning.

Control system under consideration is therefore fully magnetic: three magnetorquers and one magnetometer. This control system is by far the cheapest one. It is also among the most reliable, small and lightweight. The drawbacks are the worst accuracy and even underactuation. It is shown that control parameters and Kalman filter tuning allows accuracy of few degrees for the gravitationally unstable attitude in orbital reference frame. Inertia tensor uncertainty, unaccounted disturbance and magnetometer bias influence is assessed also.

1. Problem statement

Rigid spacecraft angular motion is considered. The satellite is equipped with three mutually orthogonal magnetorquers and three-axis magnetometer.

Magnetorquers are capable to produce any restricted dipole moment. Disturbing torques include gravitational and unaccounted ones. The latter is represented by constant and/or arbitrary Gaussian value. Inertia tensor knowledge is also erroneous.

Satellite and its orbit parameters are as follows:

- circular orbit, altitude 1000 *km*, inclination 82.5°, Earth radius 6371 *km*;
- principal moments of inertia 5750 $kg \cdot m^2$, 2450 $kg \cdot m^2$, 4000 $kg \cdot m^2$;
- unaccounted disturbing torque value is $\pm 5 \cdot 10^{-4}$ $N \cdot m$;
- magnetometer parameters: sensing range for each channel ±60000 *nT*, maximum absolute error is 100 *nT*;
- maximum dipole moment for each magnetorquer is 250 $A \cdot m^2$.

Following reference frames are used:

$OX_0Y_0Z_0$ is orbital reference frame located at the satellite center of mass. OX_0 is directed along the satellite radius-vector, OY_0 is directed towards the orbital motion and lies in orbital plane, OZ_0 completes the frame to be right-handed;

OXYZ is bound frame described by principal axes of inertia.

Satellite attitude is represented using Euler angles φ, ψ, θ (rotation sequence 1-3-2). Direction cosines matrix $\mathbf{A}$ for transition from $OX_0Y_0Z_0$ frame to *OXYZ* is

$$\mathbf{A} = \begin{pmatrix} \cos\varphi\cos\theta & \cos\varphi\sin\theta\cos\psi + \sin\varphi\sin\psi & \cos\varphi\sin\theta\sin\psi - \sin\varphi\cos\psi \\ -\sin\theta & \cos\theta\cos\psi & \cos\theta\sin\psi \\ \sin\varphi\cos\theta & \sin\varphi\sin\theta\cos\psi - \cos\varphi\sin\psi & \sin\varphi\sin\theta\sin\psi + \cos\varphi\cos\psi \end{pmatrix}. \quad (1.1)$$

Satellite motion is modelled using Euler dynamical equations and kinematic relations based on Euler angles φ, ψ, θ, direction cosines matrix $\mathbf{A}$ elements a_{ij} (both used for analytical study) and quaternion $\Lambda = (\mathbf{q}, q_0)$ (used for numerical simulation). Satellite state vector comprises of angular velocity components and relevant positional parameters. Angular velocity may represent either absolute motion ($\boldsymbol{\omega}$ and its components $\omega_1, \omega_2, \omega_3$) or relative motion with respect to orbital reference frame ($\boldsymbol{\Omega}$ and $\Omega_1, \Omega_2, \Omega_3$). Absolute and relative velocities are related by

$$\boldsymbol{\omega} = \boldsymbol{\Omega} + \mathbf{A}\boldsymbol{\omega}_{orb} \quad (1.2)$$

where $\boldsymbol{\omega}_{orb}$ is orbital reference frame angular velocity. Circular orbit leads to $\boldsymbol{\omega}_{orb} = (0, 0, \omega_0)$.

Dynamical Euler equations for the satellite with arbitrary inertia tensor $\mathbf{J}_x = \mathrm{diag}(A, B, C)$ are

$$\mathbf{J}\dot{\boldsymbol{\omega}} + \boldsymbol{\omega} \times \mathbf{J}\boldsymbol{\omega} = \mathbf{M} \quad (1.3)$$

for absolute angular velocity and

$$\mathbf{J}\dot{\boldsymbol{\Omega}} + \boldsymbol{\Omega} \times \mathbf{J}\boldsymbol{\Omega} = \mathbf{M} + \mathbf{M}_{rel} \quad (1.4)$$

where

$$\mathbf{M}_{rel} = -\mathbf{JWA}\boldsymbol{\omega}_{orb} - \boldsymbol{\Omega} \times \mathbf{JA}\boldsymbol{\omega}_{orb} - \mathbf{A}\boldsymbol{\omega}_{orb} \times \mathbf{J}(\boldsymbol{\Omega} + \mathbf{A}\boldsymbol{\omega}_{orb}),$$

$$\mathbf{W}=\begin{pmatrix} 0 & \omega_3 & -\omega_2 \\ -\omega_3 & 0 & \omega_1 \\ \omega_2 & -\omega_1 & 0 \end{pmatrix} \tag{1.5}$$

for relative angular velocity.

The torque may contain control part $\mathbf{M}_{ctrl}$ and disturbing part. The latter is divided into gravitational and unaccounted one so $\mathbf{M}=\mathbf{M}_{ctrl}+\mathbf{M}_{gr}+\mathbf{M}_{dist}$.

Dynamical equations are supplemented with kinematic relations. Quaternion kinematics is

$$\begin{pmatrix} \dot{\mathbf{q}} \\ \dot{q}_0 \end{pmatrix}=\frac{1}{2}\mathbf{C}\begin{pmatrix} \mathbf{q} \\ q_0 \end{pmatrix}, \tag{1.6}$$

$$\mathbf{C}=\begin{bmatrix} 0 & \omega_3 & -\omega_2 & \omega_1 \\ -\omega_3 & 0 & \omega_1 & \omega_2 \\ \omega_2 & -\omega_1 & 0 & \omega_3 \\ -\omega_1 & -\omega_2 & -\omega_3 & 0 \end{bmatrix}.$$

Direction cosines matrix is used for control construction, in this case

$$\dot{\mathbf{A}}=\mathbf{W}\mathbf{A}. \tag{1.7}$$

Euler angles are used for analytical analysis, in this case

$$\begin{aligned} \dot{\psi} &= \frac{1}{\cos\theta}\left(\Omega_1\cos\varphi+\Omega_3\sin\varphi\right), \\ \dot{\theta} &= \Omega_3\cos\varphi-\Omega_1\sin\varphi, \\ \dot{\varphi} &= \Omega_2+\operatorname{tg}\theta\left(\Omega_1\cos\varphi+\Omega_3\sin\varphi\right) \end{aligned} \tag{1.8}$$

for relative angular velocity.

Control torque is

$$\mathbf{M}_{ctrl}=\mathbf{m}\times\mathbf{B}$$

where $\mathbf{m}$ is dipole control moment of the satellite, $\mathbf{B}$ is geomagnetic induction vector in bound frame. Gravitational torque is

$$\mathbf{M}_{gr}=3\omega_0^2\left(\mathbf{A}\mathbf{e}_1\right)\times\mathbf{J}\left(\mathbf{A}\mathbf{e}_1\right) \tag{1.9}$$

where $\mathbf{e}_1=\left(1,0,0\right)^T$ is satellite radius-vector in orbital frame.

Unaccounted disturbing torque is modelled using three different approaches. Gaussian distribution allows modelling arbitrary disturbances with negligible effect on satellite motion since control torque is few orders greater. Constant disturbance on the level of $10^{-4}\,N{\cdot}m$ augmented with Gaussian one represents more important disturbance. Constant torque may arise due to aerodynamic or solar pressure torques acting on satellite with vast solar panels. The worst case is constant torque of $5{\cdot}10^{-4}\,N{\cdot}m$ value.

Inclined dipole model is mainly used to represent geomagnetic field. Common IGRF/WMM models have two drawbacks. They cannot be used for the altitude

considered and require extensive computation. Inclined dipole allows quite accurate field representation paired with simple computational procedures. Geomagnetic induction vector is

$$\mathbf{B} = \frac{\mu_e}{r^5}\left(\mathbf{k}r^2 - 3(\mathbf{kr})\mathbf{r}\right)$$

where $\mathbf{k}$ is Earth dipole vector and $\mathbf{r}$ is satellite radius-vector. Even more simple model is used for analytical analysis. Considering direct dipole geomagnetic induction vector may be written in orbital frame in compact form

$$\mathbf{B}_{orb} = B_0 \begin{pmatrix} -2\sin u \sin i \\ \cos u \sin i \\ \cos i \end{pmatrix} \qquad (1.10)$$

where $B_0 = \frac{\mu_e}{r^3}$, $\mu_e = 7.812 \cdot 10^6 km^3 \cdot kg \cdot s^{-2} \cdot A^{-1}$, r is satellite radius vector magnitude. Geomagnetic induction measurements are modelled as

$$\begin{aligned} &\tilde{\mathbf{B}} = \mathbf{A}\mathbf{B}_{orb} + \Delta\mathbf{B} + \boldsymbol{\eta}_{\mathbf{B}}, \\ &\Delta\dot{\mathbf{B}} = \boldsymbol{\eta}_{\Delta\mathbf{B}} \end{aligned} \qquad (1.11)$$

where $\tilde{\mathbf{B}}$ are magnetometer readings, $\mathbf{B}_{orb}$ is modelled induction (inclined field is used in Kalman filter), $\Delta\mathbf{B}$ is magnetometer bias, $\boldsymbol{\eta}_{\mathbf{B}}$ and $\boldsymbol{\eta}_{\Delta\mathbf{B}}$ are Gaussian magnetometer error and bias rate of change, each with zero mean ($\mathrm{M}\langle\boldsymbol{\eta}_{\mathbf{B}}\rangle = 0$ and $\mathrm{M}\langle\boldsymbol{\eta}_{\Delta\mathbf{B}}\rangle = 0$).

2. Attitude reconstruction using magnetometer

Kalman filter basics

Kalman filter is a recursive algorithm that uses dynamical system model and sensor readings for actual motion reconstruction. For discrete readings at time steps t_k state vector assumption $\hat{\mathbf{x}}_k = \hat{\mathbf{x}}(t_k)$ is calculated. Discrete Kalman filter utilizes correction of previous estimate [12,13]. Consider step $k-1$ along with corresponding state vector estimation $\hat{\mathbf{x}}_{k-1}^+$ and covariance matrix P_{k-1}^+. The goal is to find state vector estimate for the next step $\hat{\mathbf{x}}_k^+$. First a priory estimate $\hat{\mathbf{x}}_k^-$ is formed using mathematical model integration. It is corrected using measurements vector $\mathbf{z}_k$ to obtain a posteriori estimate $\hat{\mathbf{x}}_k^+$. Covariance error matrix P_k^- is constructed from the previous step information using Riccati equation. Measurements allow updated covariance matrix P_k^+.

Kalman filter is designed for linear mathematical models and allows the best mean-square state vector estimate. It may be adapted for any non-linear mathematical models of both dynamical system and measurements,

$$\dot{\mathbf{x}}(t) = \mathbf{f}(\mathbf{x}, t) + \mathbf{w}(t), \qquad (2.1)$$

$$\dot{\mathbf{z}}(t)=\mathbf{h}(\mathbf{x},t)+\mathbf{v}(t) \qquad (2.2)$$

where $\mathbf{w}(t)$ is Gaussian dynamical model error with covariance matrix $\mathbf{Q}$, $\mathbf{v}(t)$ is Gaussian measurements error with covariance matrix $\mathbf{R}$.

Kalman filter requires right-side functions $\mathbf{f}(\mathbf{x},t)$ and $\mathbf{h}(\mathbf{x},t)$ decomposition into Taylor series in the vicinity of current state vector. Only linear terms are used in the filter. Dynamical system and measurements model matrices are

$$\mathbf{F}_k=\left.\frac{\partial\mathbf{f}(\mathbf{x},t)}{\partial\mathbf{x}}\right|_{\mathbf{x}=\hat{\mathbf{x}}_k^-,t=t_k},\ \mathbf{H}_k=\left.\frac{\partial\mathbf{h}(\mathbf{x},t)}{\partial\mathbf{x}}\right|_{\mathbf{x}=\hat{\mathbf{x}}_k^-,t=t_k}. \qquad (2.3)$$

Discrete extended Kalman filter uses non-linear dynamical and measurements models for a priory estimate prediction and a posteriori correction [14].

Prediction phase is

$$\hat{\mathbf{x}}_k^-=\int_{t_{k-1}}^{t_k}\mathbf{f}\left(\hat{\mathbf{x}}_{k-1}^+,t\right)dt,$$
$$\mathbf{P}_k^-=\mathbf{\Phi}_k\mathbf{P}_{k-1}^+\mathbf{\Phi}_k^{\mathrm{T}}+\mathbf{Q}_k. \qquad (2.4)$$

Correction phase is

$$\mathbf{K}_k=\mathbf{P}_k^-\mathbf{H}_k^{\mathrm{T}}\left(\mathbf{H}_k\mathbf{P}_k^-\mathbf{H}_k^{\mathrm{T}}+\mathbf{R}_k\right)^{-1},$$
$$\hat{\mathbf{x}}_k^+=\hat{\mathbf{x}}_k^-+\mathbf{K}_k\left(\mathbf{z}_k-\mathbf{h}\left(\hat{\mathbf{x}}_k^-,t_k\right)\right), \qquad (2.5)$$
$$\mathbf{P}_k^+=\left(\mathbf{E}-\mathbf{K}_k\mathbf{H}_k\right)\mathbf{P}_k^-$$

where $\mathbf{\Phi}_k$ is transition matrix between states for steps $k-1$ and k, $\mathbf{E}$ is identity matrix, $\mathbf{K}$ is weighing matrix.

We now construct Kalman filter to obtain satellite attitude in the orbital reference frame. State vector is

$$\mathbf{x}=\left(\mathbf{q}\ \boldsymbol{\omega}\right).$$

Dynamical model of controlled satellite angular motion is

$$\mathbf{J}\dot{\boldsymbol{\omega}}=\mathbf{m}\times\mathbf{B}+3\omega_0^2\mathbf{A}\mathbf{e}_1\times\mathbf{J}\mathbf{A}\mathbf{e}_1-\boldsymbol{\omega}\times\mathbf{J}\boldsymbol{\omega}, \qquad (2.6)$$

so Gaussian disturbance is not taken into account. Quaternion kinematics (1.6) is used.

Equations linearization

Dynamical equations and kinematics should be linearized in the vicinity of current state vector. Rewrite equations (1.6)-(2.6) as

$$\frac{d}{dt}\delta\mathbf{x}(t)=\mathbf{F}(t)\delta\mathbf{x}(t) \qquad (2.7)$$

where $\delta\mathbf{x}(t)$ is small state vector increment, $\mathbf{F}(t)$ is matrix of equations of motion linearized in the vicinity of current state. State vector $\mathbf{x}(t)$ can be divided into the estimated part $\hat{\mathbf{x}}(t)$ and misalignment $\delta\mathbf{x}(t)$,

$$\mathbf{x}(t)=\hat{\mathbf{x}}(t)+\delta\mathbf{x}(t). \qquad (2.8)$$

In order to linearize kinematic relations (1.6) note that quaternion sum in (2.8) actually means sum of rotations which is represented by quaternion multiplication $\Lambda=\delta\Lambda\circ\hat{\Lambda}$.

Taking derivative and remembering (1.6) leads to

$$\dot{\Lambda}=\delta\dot{\Lambda}\circ\hat{\Lambda}+\delta\Lambda\circ\dot{\hat{\Lambda}}=\frac{1}{2}\mathbf{C}\delta\Lambda\circ\hat{\Lambda}.$$

Introduce kinematics for the quaternion estimate $\hat{\Lambda}$,

$$\delta\dot{\Lambda}\circ\hat{\Lambda}+\delta\Lambda\circ\frac{1}{2}\hat{\mathbf{C}}\hat{\Lambda}=\frac{1}{2}\mathbf{C}\delta\Lambda\circ\hat{\Lambda}.$$

The latter expression may be multiplied with inverse quaternion $\hat{\Lambda}^{-1}$. Note that $\hat{\Lambda}\circ\hat{\Lambda}^{-1}=e$ where e has null vector part. Taking into account $\mathbf{C}=\hat{\mathbf{C}}+\delta\mathbf{C}$ we get

$$\delta\dot{\Lambda}=-\delta\Lambda\circ\frac{1}{2}\mathbf{C}e+\delta\Lambda\circ\frac{1}{2}\delta\mathbf{C}e+\frac{1}{2}\mathbf{C}\delta\Lambda$$

or

$$2\delta\dot{\Lambda}=\begin{pmatrix}-\mathbf{W} & \mathbf{\Omega}\\ -\mathbf{\Omega}^T & 0\end{pmatrix}\delta\Lambda+\begin{pmatrix}-\delta\mathbf{W} & \delta\mathbf{\Omega}\\ -\delta\mathbf{\Omega}^T & 0\end{pmatrix}\delta\Lambda-\begin{pmatrix}\mathbf{W} & \mathbf{\Omega}\\ -\mathbf{\Omega}^T & 0\end{pmatrix}\delta\Lambda.$$

Omitting second order small terms and assuming unit scalar part for $\delta\Lambda=\begin{pmatrix}\delta\mathbf{q} & 1\end{pmatrix}$ we get linearized kinematic relations

$$\delta\dot{\mathbf{q}}=-\mathbf{W}\delta\mathbf{q}+\frac{1}{2}\delta\mathbf{\Omega},$$
$$\delta\dot{q}_0=0. \qquad (2.9)$$

Expression (2.9) is further rewritten as

$$\delta\dot{\mathbf{q}}=-\mathbf{W}\delta\mathbf{q}+\mathbf{W}_{A\omega_0}\delta\mathbf{q}+\frac{1}{2}\delta\boldsymbol{\omega}-\frac{1}{2}\delta\left(\mathbf{A}\boldsymbol{\omega}_0\right)$$

where $\mathbf{W}_{\mathbf{A}\boldsymbol{\omega}_0}$ is a skew symmetric matrix of vector $\mathbf{A}\boldsymbol{\omega}_0$ analogous to (1.5).

Taking into account constant orbital angular velocity we get

$$\delta\left(\mathbf{A}\boldsymbol{\omega}_0\right)=\mathbf{A}\left(\delta\mathbf{q}\right)\mathbf{A}\left(\hat{\mathbf{q}}\right)\boldsymbol{\omega}_0.$$

Using relation between small rotation matrix $\mathbf{A}$ and quaternion $\mathbf{A}\left(\delta\mathbf{q}\right)=\mathbf{E}-2\mathbf{W}_{\delta\mathbf{q}}$ rewrite the latter expression as

$$\delta\left(\mathbf{A}\boldsymbol{\omega}_0\right)=2\mathbf{W}_{\mathbf{A}(\hat{\mathbf{q}})\boldsymbol{\omega}_0}\delta\mathbf{q}.$$

Omitting difference between $\mathbf{A}\left(\mathbf{q}\right)\boldsymbol{\omega}_0$ and $\mathbf{A}\left(\hat{\mathbf{q}}\right)\boldsymbol{\omega}_0$ finally leads to the linearized kinematics

$$\delta\dot{\mathbf{q}}=-\mathbf{W}\delta\mathbf{q}+\frac{1}{2}\delta\boldsymbol{\omega}. \qquad (2.10)$$

Linearization of dynamical equations (2.6) involves gravitational torque (1.9) in the form

$$\mathbf{M}_{gr} = 3\omega_0^2 \mathbf{A}(\Lambda)\mathbf{e}_1 \times \mathbf{J}\mathbf{A}(\Lambda)\mathbf{e}_1.$$

We use small rotation in the vicinity of current estimate given with the direction cosines matrix,

$$\mathbf{A}(\Lambda) = \mathbf{A}\left(\delta\Lambda\hat{\Lambda}\right) = \mathbf{A}(\delta\Lambda)\mathbf{A}\left(\hat{\Lambda}\right).$$

This leads to

$$\delta\mathbf{M}_{gr} = 3\omega_0^2\left(\mathbf{W}_{\mathbf{e}_1}\mathbf{J}\mathbf{W}_{\mathbf{e}_1} - \mathbf{W}_{\mathbf{J}\mathbf{e}_1}\mathbf{W}_{\mathbf{e}_1}\right)\delta\boldsymbol{\lambda}.$$

Finally linearized gravitational torque is

$$\delta\mathbf{M}_{gr} = 6\omega_0^2\mathbf{F}_{gr}\delta\boldsymbol{\lambda} \qquad (2.11)$$

where

$$\mathbf{F}_{gr} = \begin{pmatrix} \left(e_y^2 - e_z^2\right)(B-C) & -e_x e_y (B-C) & e_z e_x (B-C) \\ e_x e_y (C-A) & \left(e_z^2 - e_x^2\right)(C-A) & -e_z e_y (C-A) \\ -e_x e_z (A-B) & e_y e_z (A-B) & \left(e_x^2 - e_y^2\right)(A-B) \end{pmatrix},$$

e_x, e_y, e_z are unit radius-vector components in bound frame.

Gyroscopic torque is

$$\mathbf{M}_{gir} = -\boldsymbol{\omega} \times \mathbf{J}\boldsymbol{\omega}.$$

Linearization leads to

$$\delta\mathbf{M}_{gir} = \mathbf{F}_{gir}\delta\boldsymbol{\omega} \qquad (2.12)$$

where

$$\mathbf{F}_{gir} = \begin{pmatrix} 0 & \omega_3(B-C) & \omega_2(B-C) \\ \omega_3(C-A) & 0 & \omega_1(C-A) \\ \omega_2(A-B) & \omega_1(A-B) & 0 \end{pmatrix},$$

Control torque $\mathbf{M}$ is the last one to be linearized in the vicinity of current estimate $\hat{\Lambda}$,

$$\mathbf{M} = \delta\mathbf{M} + \hat{\mathbf{M}} = \mathbf{m} \times \mathbf{A}\left(\delta\Lambda \circ \hat{\Lambda}\right)\mathbf{B}_{orb}.$$

Note that rotation matrix of two quaternions multiplication is a multiplication of two rotation matrices,

$$\mathbf{A}\left(\delta\Lambda \circ \hat{\Lambda}\right) = \mathbf{A}(\delta\Lambda)\mathbf{A}\left(\hat{\Lambda}\right). \qquad (2.13)$$

Suppose that $\delta\Lambda$ has unit scalar part, $\delta\Lambda = \left(1\ \delta\mathbf{q}\right)$. This allows approximate expression

$$\mathbf{A}(\delta\Lambda) = \mathbf{E} - 2\mathbf{W}_{\delta\mathbf{q}} \qquad (2.14)$$

and control torque

$$\delta\mathbf{M} = \mathbf{m} \times \left(-2\mathbf{W}_{\delta\mathbf{q}}\mathbf{A}\left(\hat{\Lambda}\right)\mathbf{B}_{orb}\right) = \mathbf{m} \times \left(-2\mathbf{W}_{\delta\mathbf{q}}\hat{\mathbf{B}}\right) = \mathbf{m} \times \left(2\mathbf{W}_{\hat{\mathbf{B}}}\delta\mathbf{q}\right) = 2\mathbf{W}_{\mathbf{m}}\mathbf{W}_{\hat{\mathbf{B}}}\delta\mathbf{q} \qquad (2.15)$$

where $\mathbf{W_m}$ and $\mathbf{W_{\hat{B}}}$ are skew symmetric matrices of control dipole moment and geomagnetic induction vector estimates.

Linearized equations are finally

$$\frac{d}{dt}\delta\mathbf{x}(t)=\mathbf{F}(t)\delta\mathbf{x}(t)$$

where dynamics matrix $\mathbf{F}$ is introduced using (2.10), (2.11), (2.12) and (2.15) as

$$\mathbf{F}=\begin{pmatrix} -\mathbf{W} & \frac{1}{2}\mathbf{E} \\ \mathbf{J}^{-1}\left(6\omega_0^2\mathbf{F}_{gr}+2\mathbf{W_m}\mathbf{W_{\hat{B}}}\right) & \mathbf{J}^{-1}\mathbf{F}_{gir} \end{pmatrix}. \qquad (2.16)$$

Magnetometer measurements model is

$$\mathbf{z}=\mathbf{A}\mathbf{B}_{orb}+\boldsymbol{\eta}_{\mathbf{B}} \qquad (2.17)$$

where $\boldsymbol{\eta}_{\mathbf{B}}$ is Gaussian geomagnetic induction vector error with zero mean. Linearized measurements model (2.17) is

$$\mathbf{z}=\delta\mathbf{z}+\hat{\mathbf{z}}=\mathbf{A}\left(\delta\Lambda\hat{\Lambda}\right)\mathbf{B}_{orb}.$$

Using (2.13) and (2.14) we get

$$\delta\mathbf{z}=2\mathbf{W}_{\delta\mathbf{q}}\hat{\mathbf{B}}=2\mathbf{W}_{\hat{\mathbf{B}}}\delta\mathbf{q}.$$

and measurements matrix is

$$\mathbf{H}=2\mathbf{W}_{\hat{\mathbf{B}}}. \qquad (2.18)$$

Kalman filter simulation

Kalman filter performance is modelled with control taken into account. Kalman filter initialization requires covariance matrices of measurements errors $\mathbf{R}$, model errors $\mathbf{Q}$ and initial matrix of state vector estimation errors $\mathbf{P}_0$.

Magnetometer error is initially limited to σ_{meas}=100 *nT*. This error should be increased to take into account possible geomagnetic field model error that is about 200 *nT* [15] for IGRF model. This leads to the error σ_{meas}=300 *nT*. Measurements error covariance matrix is

$$\mathbf{R}=diag\left(\sigma_{meas}^2,\sigma_{meas}^2,\sigma_{meas}^2\right).$$

Unaccounted disturbing torque is supposed to be of the order of $D=5\cdot10^{-4}N\cdot m$. Consider it to have Gaussian distribution with zero mean. The satellite dynamics is subjected to the error

$$\sigma_\omega=I^{-1}\cdot D\cdot\Delta t \qquad (2.19)$$

where I is the smallest inertia moment, Δt is measurements sampling interval. Kinematic relations are subject to the error

$$\sigma_q=I^{-1}\cdot D\cdot\Delta t^2/2.$$

Assuming no correlation between these errors we introduce mathematical model errors covariance matrix

$$\mathbf{Q} = diag\left(\sigma_q^2, \sigma_q^2, \sigma_q^2, \sigma_\omega^2, \sigma_\omega^2, \sigma_\omega^2\right). \qquad (2.20)$$

Initial state vector estimate is arbitrary. Suppose it to be zeroed (unit quaternion for no rotation and no angular velocity). Consider maximum angle error $\sigma_{q_0} = \pi/2$ and knowingly big velocity error $\sigma_{\omega_0} = 10$ *deg/s*. Initial error matrix is $\mathbf{P}_0 = \left(\sigma_{q_0}^2, \sigma_{q_0}^2, \sigma_{q_0}^2, \sigma_{\omega_0}^2, \sigma_{\omega_0}^2, \sigma_{\omega_0}^2\right)$.

Chosen set of actuators and sensors involves important addition into control cycle. Magnetorquers induce magnetic field thus spoiling magnetometer readings. Two possible solutions exist. Control system may be calibrated prior to flight in order to assess magnetorquers influence on the magnetometer readings. Strong dipole moment from magnetorquers nevertheless induces errors. Another way is widely used: control and attitude determination receive their own steps in control cycle. Magnetorquers are turned off for the duration of magnetometer sampling, and its filtered reading are used for control input until next attitude determination phase. Suppose control phase to last 5 seconds while attitude determination requires only one second with magnetometer sampling rate 1 *Hz*. Initial angular velocity is 1 *deg/s*. Fig. 2.1 introduces satellite stabilization which is necessary for proper Kalman filter convergence. Stabilization time is about 5 hours. Fig. 2.2 and 2.3 bring estimation errors of angles and angular velocity. Kalman filter convergence time is about 4 hours. Satellite stabilization allowed attitude determination accuracy to exceed $\sigma = 0.2°$ and $\sigma = 7 \cdot 10^{-4}$ *deg/s*.

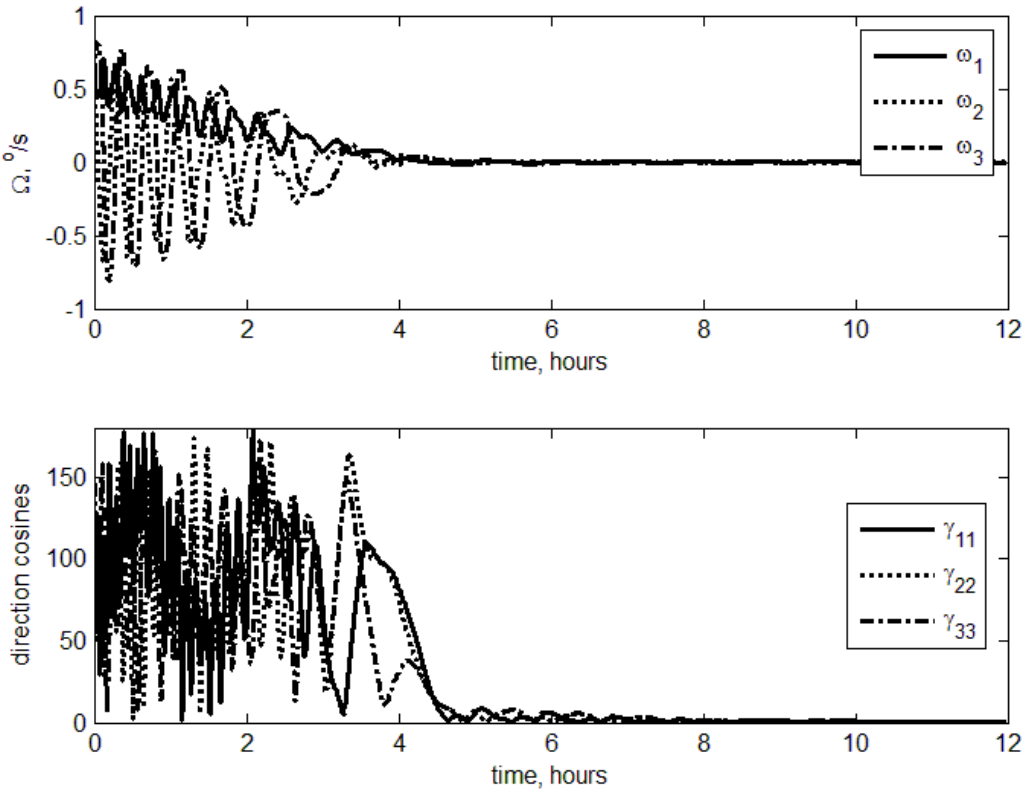

Fig. 2.1. Satellite stabilization

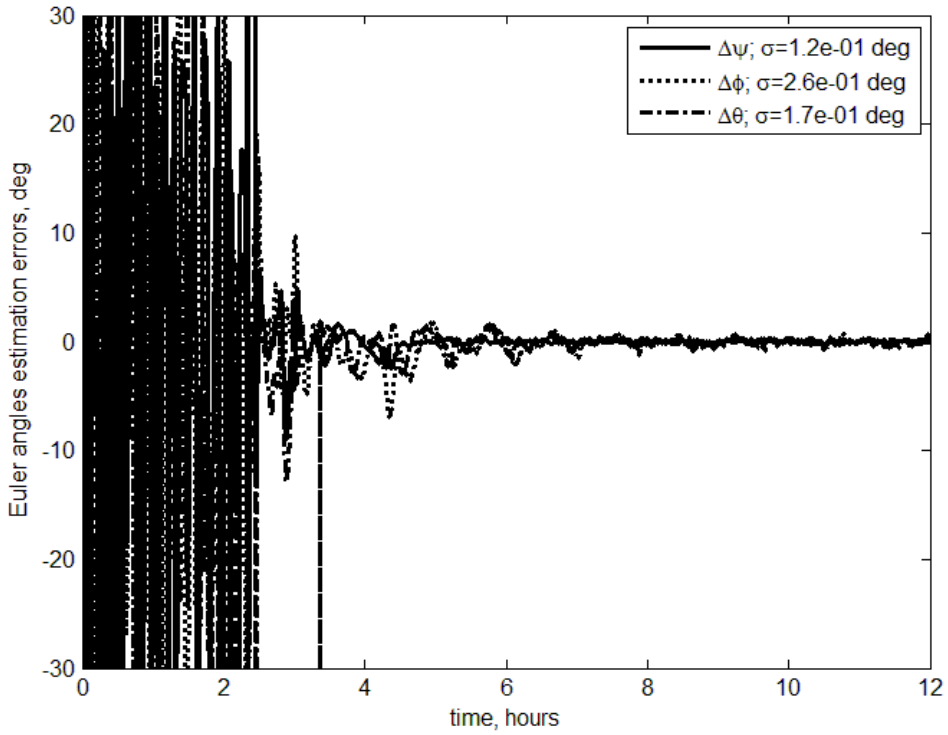

Fig. 2.2. Euler angles estimation errors

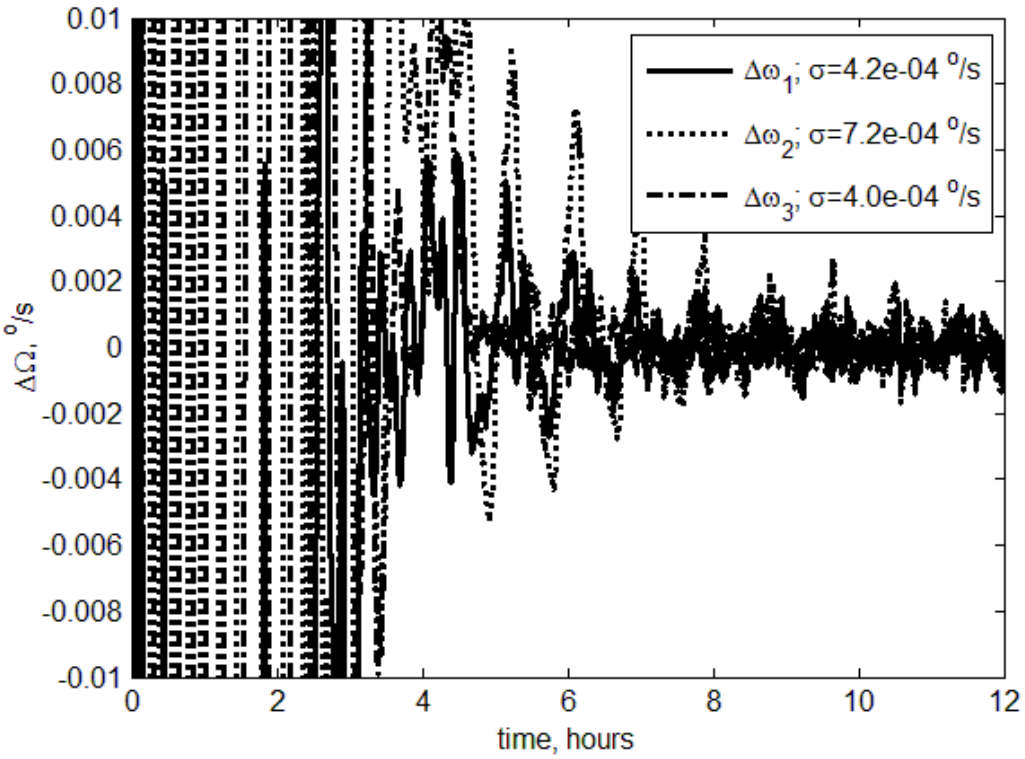

Fig. 2.3. Angular velocity estimation error

Consider now disturbing torque with constant value $D = 5 \cdot 10^{-4} N \cdot m$. This change is unaccounted in the Kalman filter. Fig. 2.4 and 2.5 represent attitude determination error for Euler angles and angular velocity. Filter convergence time increases to 7 hours. Terminal determination accuracy remains almost unchanged however with errors close to $\sigma = 0.3°$ and $\sigma = 8 \cdot 10^{-4}$ *deg/s*.

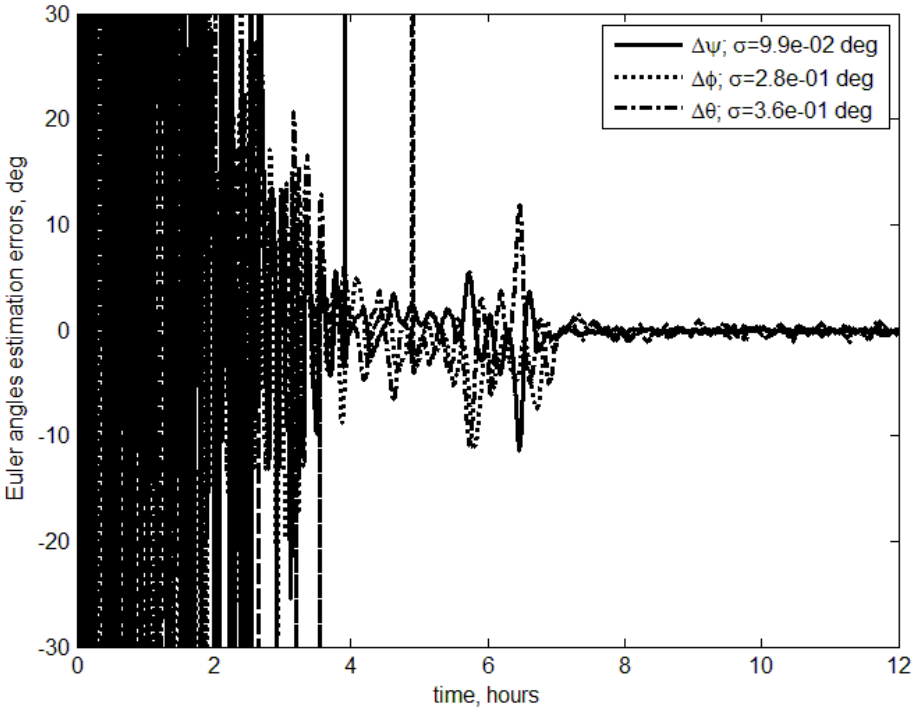

Fig. 2.4. Euler angles errors, constant disturbance

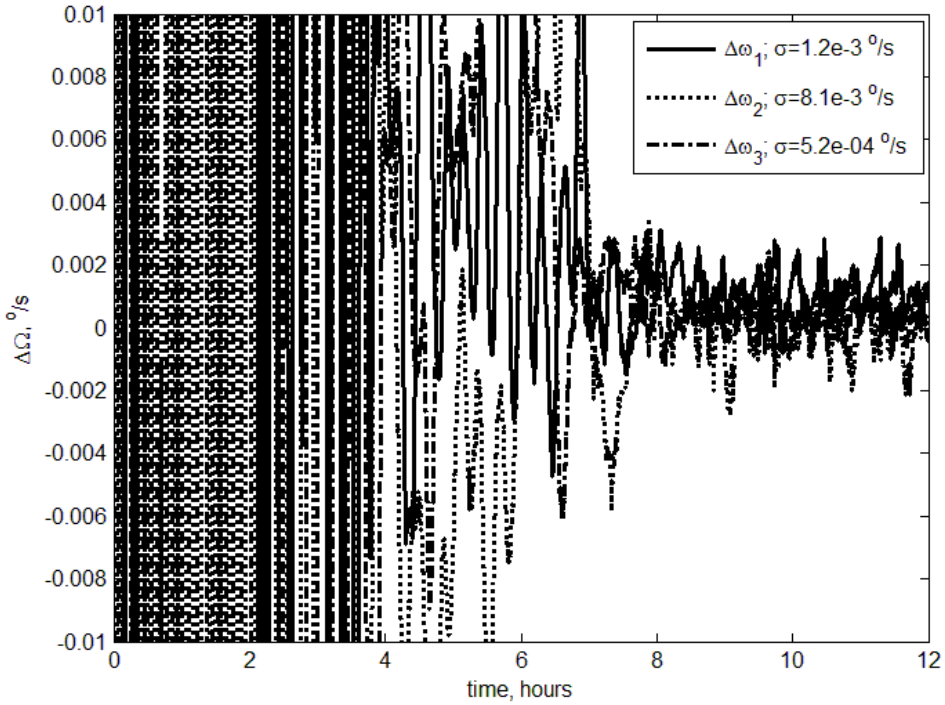

Fig. 2.5. Angular velocity errors, constant disturbance

Inertia moments of the satellite are known with maximum error of ±10% which may hinder Kalman filter performance. Following simulation is run with nominal inertia tensor $\mathbf{J}=\mathrm{diag}(5750, 2450, 4000)$ *kg·m²*. It is used in Kalman filter for the dynamical model of the satellite. However the simulation itself uses adjusted inertia tensor. At least one principal moment differs by 10% from nominal. This error has negligible impact on Kalman filter performance, both convergence time and accuracy. Even singular inertia tensor $\mathbf{J}\approx\mathrm{diag}(5836, 2468, 3600)$ *kg·m²* (one principal moment is greater than the sum of two other) leads to error of only $\sigma=0.3°$, $\sigma=8\cdot10^{-4}$ *deg/s*. Introducing constant disturbing torque of the value $D=5\cdot10^{-4}$ *N·m* with singular inertia tensor leads to error $\sigma=0.4°$ and $\sigma=1\cdot10^{-3}$ *deg/s* and convergence time 8 hours.

Magnetometer bias has almost no effect on Kalman filter performance. Bias is not taken into account in Kalman filter measurements model (2.17). Consider full model (1.11) with bias $\Delta\mathbf{B}$=100 *nT* for each channel. Fig 2.6 and 2.7 introduce angles and angular velocity estimations errors. These are around $\sigma=0.4°$ and $\sigma=8\cdot10^{-4}$ *deg/s*. These errors are not Gaussian and have periodic nature. Convergence time is about 6 hours.

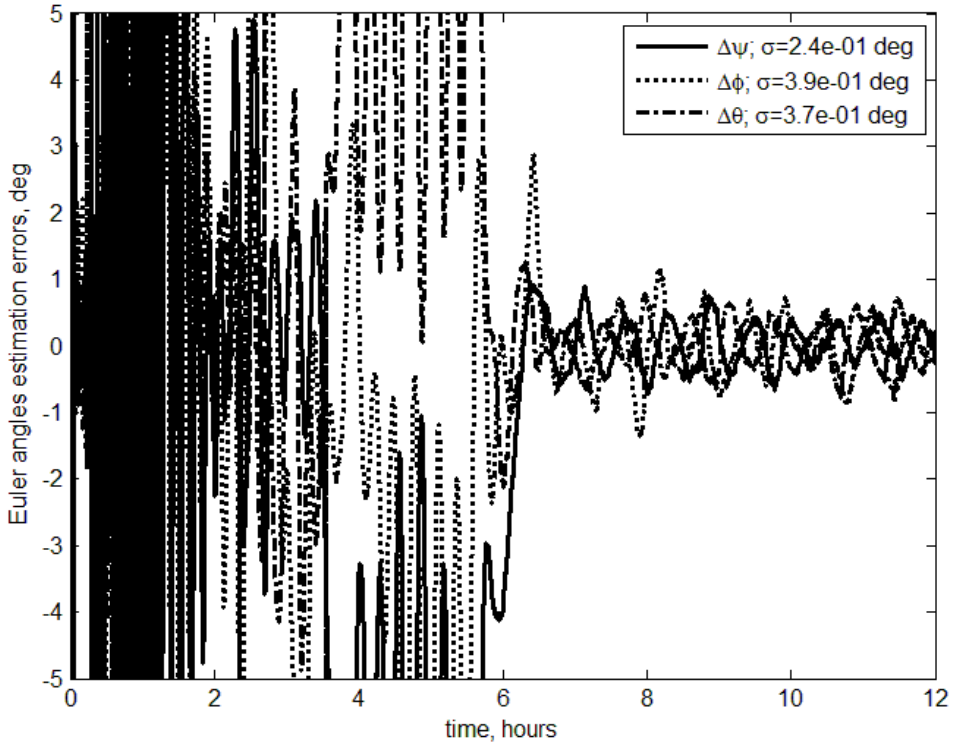

Fig. 2.6. Angles estimation errors with magnetometer bias

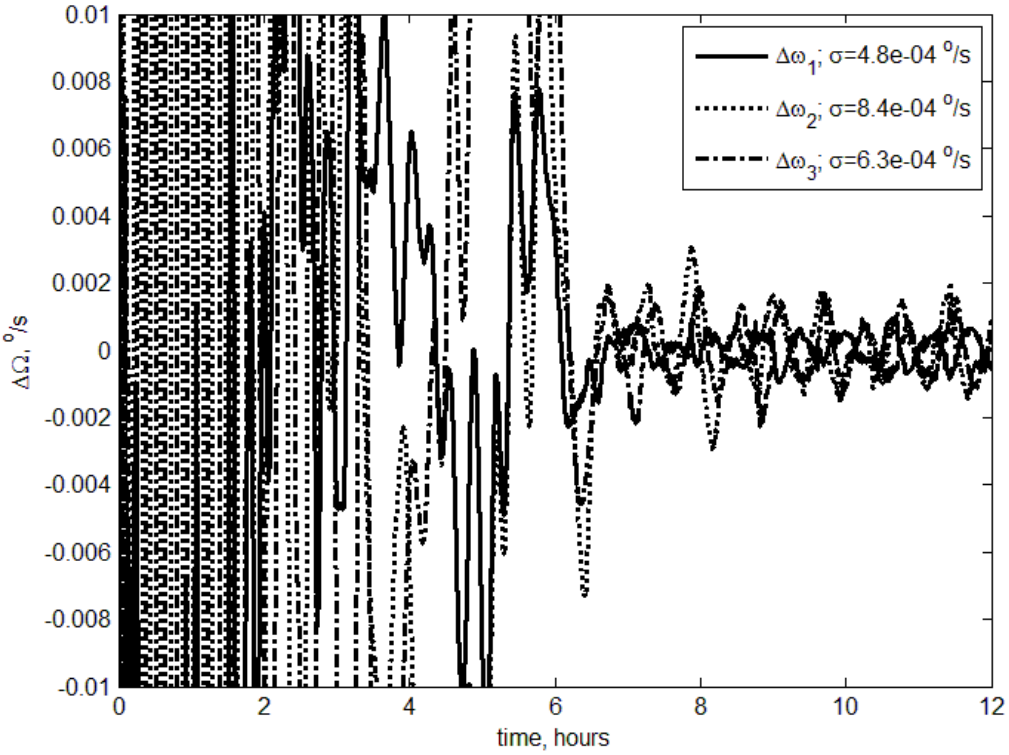

Fig. 2.7. Angular velocity estimation error with magnetometer bias

3. Attitude control using magnetorquers and magnetometer readings

Sliding mode three-axis control

Underactuation issue has one important trait for magnetorquers. Geomagnetic induction vector rotates in the inertial space. No inaccessible direction in inertial or bound reference frames exists. Any inaccessible at a moment direction will become available, but after some time. This feature allows accessible path to be constructed. This path requires perpendicular to geomagnetic induction vector torque at each control step. Finally satellite acquires necessary attitude with necessary angular velocity. Sliding control [16] may be used to obtain the above mentioned path.

Sliding control is constructed in two steps [2]. First sliding manifold $\mathbf{x}(\mathbf{\Omega},\mathbf{A},t)=0$ is constructed in phase space. Satellite motion should satisfy this relation: the satellite moves on the manifold. The manifold is constructed in such a way that necessary attitude is asymptotically stable. Sliding manifold for satellite angular motion is

$$\mathbf{x}=\lambda\mathbf{\Omega}+\mathbf{\Lambda}(\mathbf{\Omega},\mathbf{S},t)\mathbf{S}=0 \qquad (3.1)$$

where $\mathbf{S}=\begin{pmatrix}a_{23}-a_{32} & a_{31}-a_{13} & a_{12}-a_{21}\end{pmatrix}^T$ ($\mathbf{S}=0$ corresponds to diagonal direction cosines matrix) , $\mathbf{\Lambda}$ is a positive-defined variable matrix and λ is a positive value (it could be a positive-defined matrix also and even state vector function). Satellite motion on the sliding manifold is represented by $\mathbf{x}=0$. In this case attitude $\mathbf{\Omega}=0$, $\mathbf{A}=\mathbf{E}$ is asymptotically stable [2].

Control should ensure motion on the sliding manifold according to the equation

$$\dot{\mathbf{x}} = -\mathbf{J}^{-1}\mathbf{P}\mathbf{x} \qquad (3.2)$$

where $\mathbf{P}$ a is positive-defined matrix. Inertia tensor is introduced to simplify further reasoning. Taking into account (3.1) we rewrite (3.2) as

$$\dot{\lambda}\mathbf{J}\boldsymbol{\Omega} + \lambda\mathbf{J}\dot{\boldsymbol{\Omega}} + \mathbf{J}\dot{\boldsymbol{\Lambda}}\mathbf{S} + \mathbf{J}\boldsymbol{\Lambda}\dot{\mathbf{S}} = -\lambda\mathbf{P}\boldsymbol{\Omega} - \mathbf{P}\boldsymbol{\Lambda}\mathbf{S}.$$

Scalar λ characterizes damping part in control. Matrix $\boldsymbol{\Lambda}$ characterizes positional control part. Matrix $\mathbf{P}$ represents the time-response of sliding manifold acquiring. $\dot{\mathbf{S}}$ is found using (1.7). Taking into account dynamical equations (1.4) we obtain

$$\lambda\mathbf{m}\times\mathbf{B} = -\dot{\lambda}\mathbf{J}\boldsymbol{\Omega} + \lambda\left(\boldsymbol{\Omega}\times\mathbf{J}\boldsymbol{\Omega} - \mathbf{M} - \mathbf{M}_{rel}\right) - \dot{\boldsymbol{\Lambda}}\mathbf{J}\mathbf{S} - \boldsymbol{\Lambda}\left(\mathbf{J}\dot{\mathbf{S}} + \mathbf{P}\mathbf{S}\right) - \lambda\mathbf{P}\boldsymbol{\Omega}. \qquad (3.3)$$

Expression (3.3) governs magnetorquers dipole moment. Altering values of λ and $\boldsymbol{\Lambda}$ should allow the latter relation for each time and satellite attitude and velocity. The main problem is to find matrix $\boldsymbol{\Lambda}$ and its derivative. Iterative approach is considered below.

Matrix $\boldsymbol{\Lambda}$ derivative is written as

$$\dot{\boldsymbol{\Lambda}} = \frac{\boldsymbol{\Lambda}(k+1) - \boldsymbol{\Lambda}(k)}{\Delta t}$$

where Δt is control implementation step. Suppose we know satellite attitude, angular velocity and geomagnetic induction vector for $k+1$ step and previous matrix $\boldsymbol{\Lambda}(k)$. Our purpose is to find $\boldsymbol{\Lambda}(k+1)$. Rewrite (3.3) as

$$\mathbf{a} + \boldsymbol{\Lambda}(k+1)\mathbf{b} = \mathbf{m}\times\mathbf{d} \qquad (3.4)$$

where

$$\mathbf{a} = \left(-\dot{\lambda}\mathbf{J}\boldsymbol{\Omega} + \lambda\left(\boldsymbol{\Omega}\times\mathbf{J}\boldsymbol{\Omega} - \mathbf{M} - \mathbf{M}_{rel}\right) - \boldsymbol{\Lambda}\left(\mathbf{J}\dot{\mathbf{S}} + \mathbf{P}\mathbf{S}\right) - \lambda\mathbf{P}\boldsymbol{\Omega}\right)\Delta t + \boldsymbol{\Lambda}\mathbf{J}\mathbf{S},$$

$$\mathbf{b} = -\mathbf{J}\mathbf{S}, \quad \mathbf{d} = \lambda\Delta t\mathbf{B}$$

Here all indices except in $\boldsymbol{\Lambda}(k+1)$ are omitted. Set reference frame with basis vectors

$$\mathbf{e}_1 = \frac{\mathbf{d}}{|\mathbf{d}|}, \ \mathbf{e}_3 = \frac{\mathbf{d}\times\mathbf{b}}{|\mathbf{d}\times\mathbf{b}|}, \ \mathbf{e}_2 = \mathbf{e}_3\times\mathbf{e}_1.$$

Scalar product of (3.4) and $\mathbf{d}$ is

$$\left(\boldsymbol{\Lambda}(k+1)\mathbf{b}\right)\mathbf{d} = -\mathbf{a}\mathbf{d}.$$

Taking into account $\mathbf{d} = (d_1, 0, 0)^T$ and $\mathbf{b} = (b_1, b_2, 0)^T$ we get

$$\Lambda_{11}(k+1)b_1 + \Lambda_{12}(k+1)b_2 = -a_1. \qquad (3.5)$$

Matrix $\boldsymbol{\Lambda}(k+1)$ construction is performed in a few steps. First $\Lambda_{11}(k+1) > 0$ should be chosen. For example, $\Lambda_{11}(k+1) = \Lambda_{11}(k)$. This allows using (3.5) to find $\Lambda_{12}(k+1)$ and $\Lambda_{21}(k+1)$,

$$\Lambda_{12}(k+1) = \Lambda_{21}(k+1) = \left(-a_1 - \Lambda_{11}(k+1)b_1\right)/b_2 .$$

$\Lambda_{22}(k+1)$ should satisfy

$$\Lambda_{11}(k+1)\Lambda_{22}(k+1)-\Lambda_{12}^2(k+1)>0. \qquad (3.6)$$

For example $\Lambda_{22}(k+1)=\Lambda_0+\dfrac{\Lambda_{12}^2(k+1)}{\Lambda_{11}(k+1)}$, Λ_0 is some constant value. It characterizes overall positional control part. However if $\Lambda_{22}(k)$ satisfies (3.6) previous step value may be used. Finally $\Lambda_{33}(k+1)=\Lambda_{33}(k)$. Matrix $\mathbf{\Lambda}(k+1)$ is then transformed to the bound frame. Expression (3.4) is used to find control torque and dipole moment. First step values may be set as $\mathbf{\Lambda}(k+1)=\mathbf{\Lambda}(k)=\Lambda_0\mathbf{E}$.

This reasoning cannot be used in the vicinity of necessary attitude since b_1 and b_2 are close to zero. To mitigate this problem element $\Lambda_{12}(k+1)$ is constructed according to

$$\Lambda_{12}(k+1)=-\frac{a_1+\Lambda_{11}(k+1)b_1}{b_2+\delta b_2}$$

where δb_2 is small positive constant. This artificial error leads to slight discrepancy between control torque direction and possible plane perpendicular to the geomagnetic induction vector. Control torque is projected on this plane to construct dipole moment.

Iterative approach allows good results for small satellites [2]. Fig. 3.1 presents simulation results with parameters $\Lambda_0=10^{-4}$, $\delta b_2=10$, $\lambda=0.07$, $\mathbf{P}=5\mathbf{E}$, maximum control dipole moment is 2500 $A{\cdot}m^2$, control iteration step $\Delta t=1$ s. These parameters are derived from results obtained in [2].

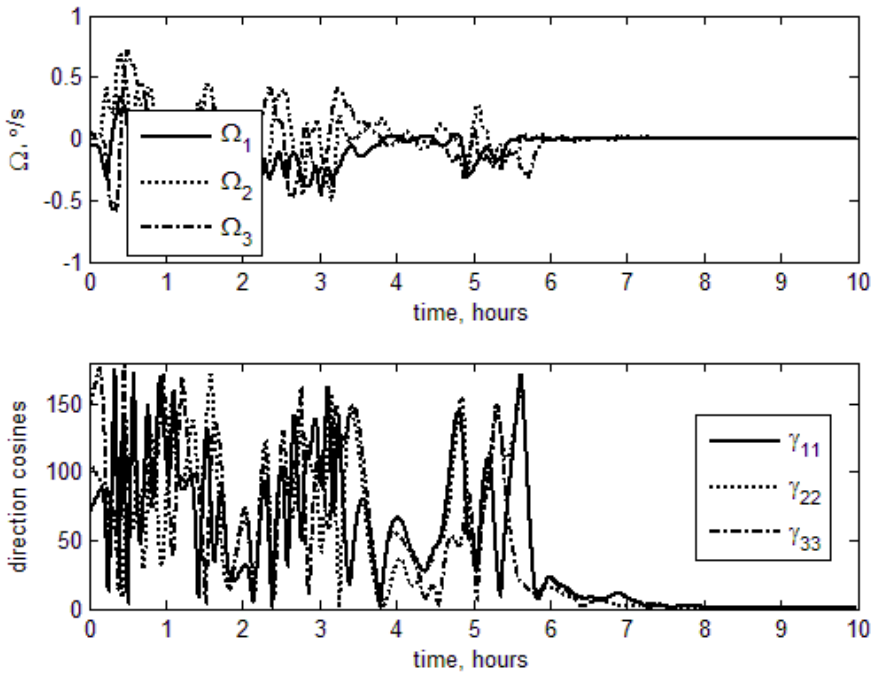

Fig. 3.1. Sliding control simulation

Magnetorquers incapable of 2500 $A{\cdot}m^2$ dipole cannot provide necessary attitude. Furthermore initial angular velocity is $\boldsymbol{\Omega}=(0.001,0.001,0.001)$ s^{-1} since faster rotation cannot be mitigated with sliding control. These drawbacks make sliding control unacceptable for three-axis magnetic attitude of big satellite.

PD-controller based control

Consider control torque based on the PD-controller [1]

$$\mathbf{m}=-k_\omega\mathbf{B}\times\boldsymbol{\omega}-k_a\mathbf{B}\times\mathbf{S}. \tag{3.7}$$

Control parameters have decisive influence on the algorithm performance. They are adjusted manually in the vicinity of optimal ones obtained using Floquet theory [17]. Equations of motion (1.4)-(1.8) are linearized in the vicinity of necessary attitude,

$$\begin{aligned}
\frac{d\Omega_1}{du}&=-k'_\omega\frac{B_0^2}{A\omega_0^2}\left[\left(B_2^2+B_3^2\right)\Omega_1-B_1B_2\Omega_2-B_1B_3\Omega_3\right]-\\
&\quad-2k_a\frac{B_0^2}{A\omega_0^2}\left[-B_1B_2\varphi-B_1B_3\theta+\left(B_2^2+B_3^2\right)\psi\right]+\Omega_2+\frac{B-C}{A}\left(\Omega_2+\psi\right),\\
\frac{d\Omega_2}{du}&=-k'_\omega\frac{B_0^2}{B\omega_0^2}\left[-B_1B_2\Omega_1+\left(B_1^2+B_3^2\right)\Omega_2-B_2B_3\Omega_3\right]-\\
&\quad-2k_a\frac{B_0^2}{B\omega_0^2}\left[\left(B_1^2+B_3^2\right)\varphi-B_2B_3\theta-B_1B_2\psi\right]-\Omega_1+\frac{C-A}{B}\left(\Omega_1-4\varphi\right),\\
\frac{d\Omega_3}{du}&=-k'_\omega\frac{B_0^2}{C\omega_0^2}\left[-B_1B_3\Omega_1-B_2B_3\Omega_2+\left(B_1^2+B_2^2\right)\Omega_3\right]-\\
&\quad-2k_a\frac{B_0^2}{C\omega_0^2}\left[-B_2B_3\varphi+\left(B_1^2+B_2^2\right)\theta-B_1B_3\psi\right]+3\frac{A-B}{C}\theta,\\
\frac{d\varphi}{du}&=\Omega_2,\qquad\frac{d\theta}{du}=\Omega_3,\qquad\frac{d\psi}{du}=\Omega_1.
\end{aligned} \tag{3.8}$$

Control parameter k_ω is substituted with $k'_\omega=k_\omega\omega_0$. This allows both parameters to have the same physical dimension. B_i are geomagnetic induction vector components in orbital reference frame, Ω_i are dimensionless relative angular velocity components, equations (3.8) utilize derivative with respect to the argument of latitude. Direct dipole model is used for geomagnetic field representations since this allows the equations (3.8) to be 2π-periodic. Floquet theory can therefore be used to analyze (3.8). Fig. 3.2 represents characteristic multipliers in the vicinity of stability area of (3.8).

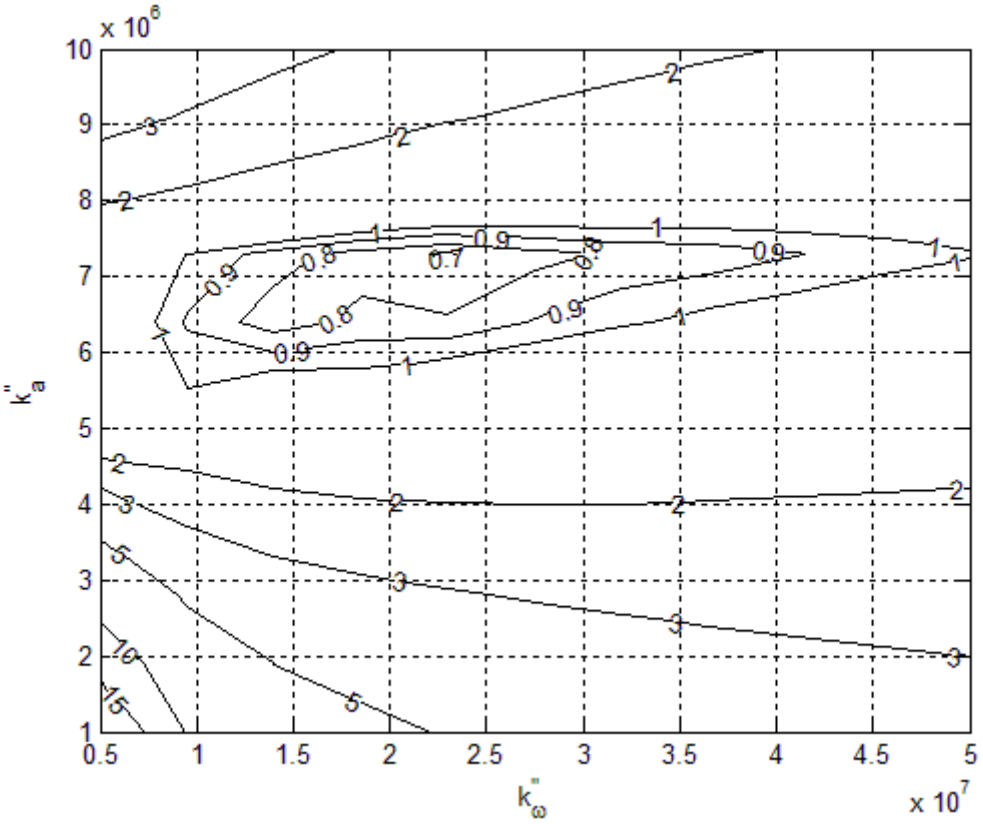

Fig. 3.2. Stability area

Results depicted on Fig. 3.2 are valid for dynamical model with a number of restrictions (linearized equations of motion, direct dipole model, unlimited dipole moment of magnetorquers). Control parameters can be found from Fig 3.2 only approximately. Manual adjustment is necessary. For the satellite considered good control parameters are $k_\omega = \frac{4\cdot 10^7}{\omega_0}\frac{N\cdot m}{T^2}$, $k_a = 1.5\cdot 10^7 \frac{N\cdot m}{T^2}$. Both control parameters are about twice as optimal ones from Fig. 3.2. Fig 3.3. bring numerical simulation result with these parameters but with accurate attitude information. Gravitational and Gaussian unaccounted disturbances are taken into account.

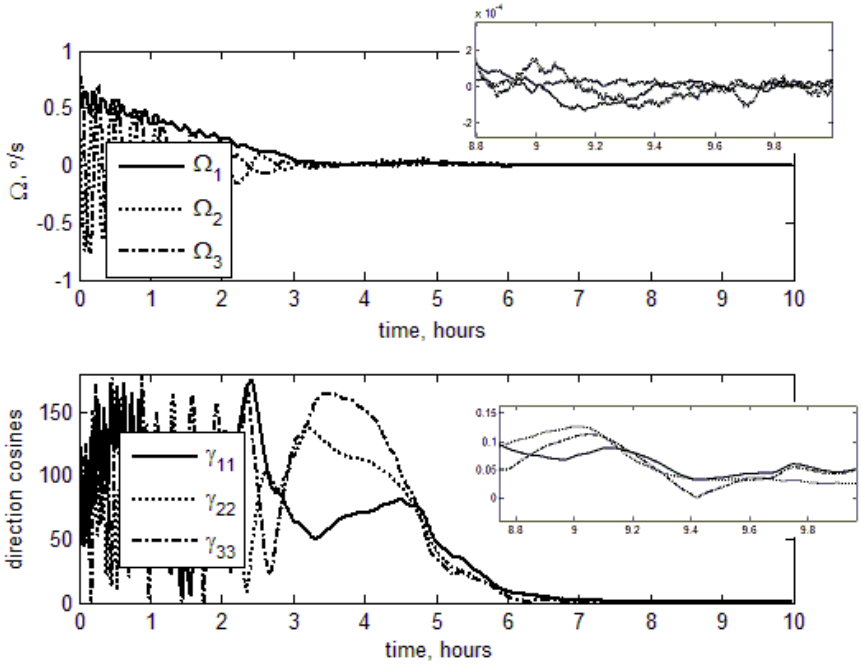

Fig. 3.3. Three-axis attitude, Gaussian disturbance

Attitude accuracy is better than 0.1°. Kalman filter simulation leads to significant accuracy decay. Worsened attitude estimation accuracy is not the only reason. Control and measurement phases rotation further hampers estimation accuracy since results valid for estimation phase are used for a number of control phases. Finally, control is completely unavailable during measurements phase. Fig 3.4 brings simulation result for Gaussian disturbance. Attitude determination phase takes 1 second, control is implemented for 5 seconds.

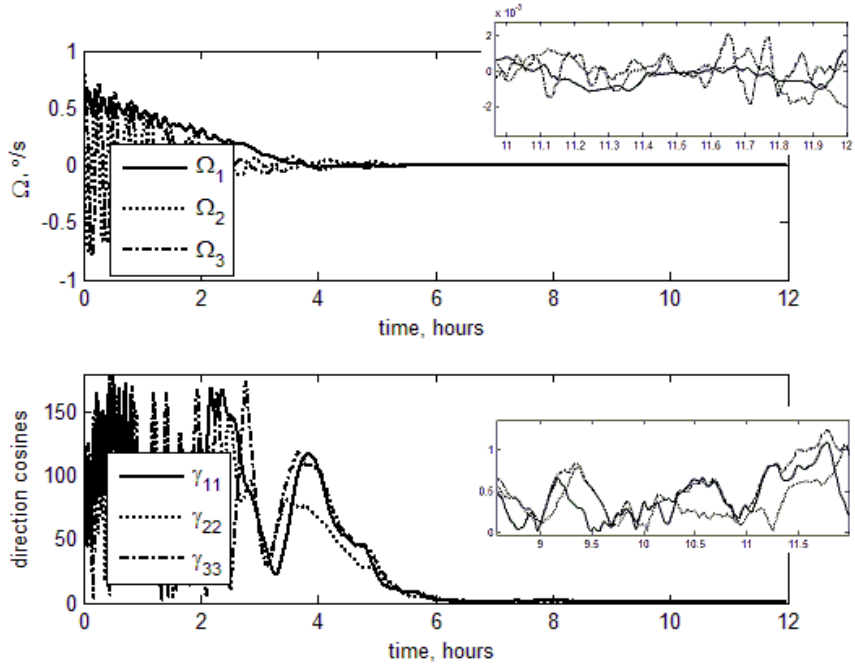

Fig. 3.4. Three-axis attitude, Kalman filter, Gaussian disturbance

Accuracy is about 1.5°. Fig. 3.5 brings the same result for combined constant and Gaussian disturbance.

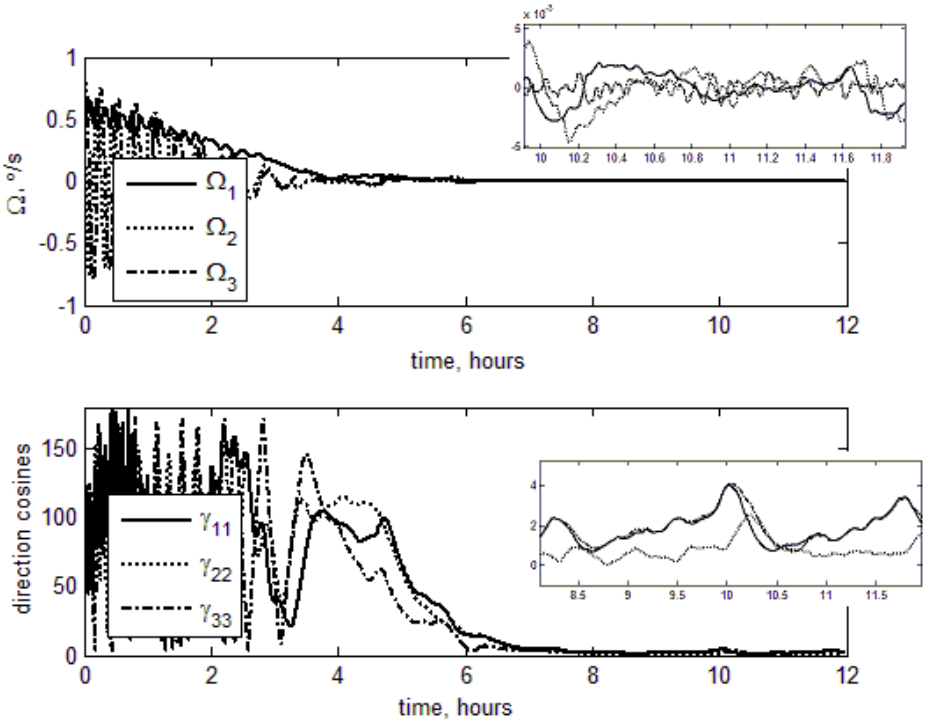

Fig. 3.5. Three-axis attitude, Kalman filter, constant and Gaussian disturbance

Accuracy is about 4°. Finally Fig. 3.6 represents simulation results with maximum constant disturbance.

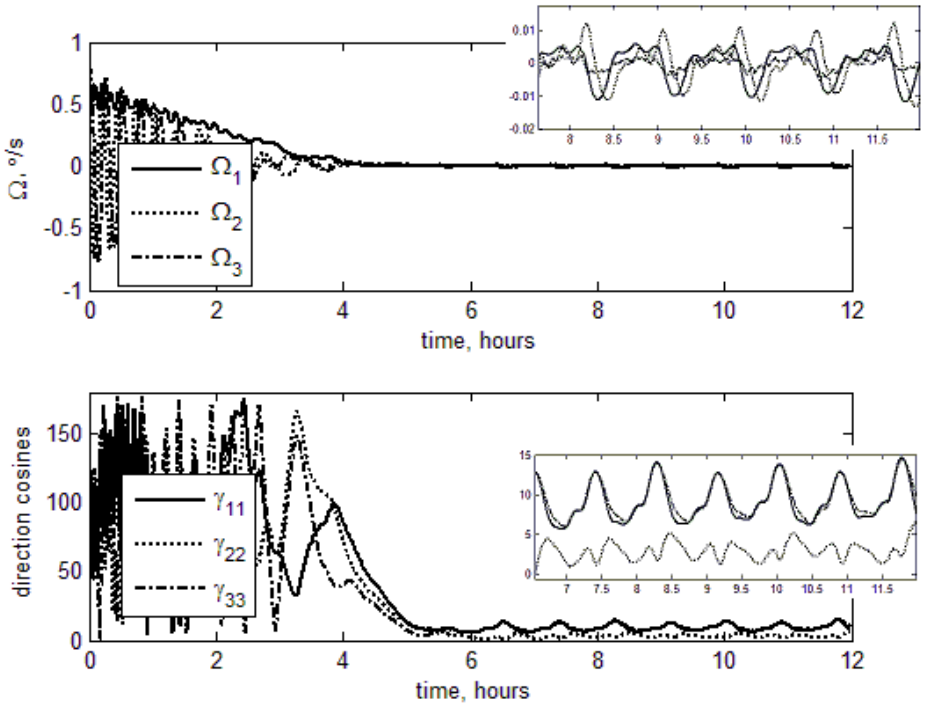

Fig. 3.6. Three-axis attitude, Kalman filter, constant disturbance

Attitude accuracy falls to 15°. Transient time is about 6 hours in all cases.

Inertia tensor inaccurate knowledge may lead to significant errors in attitude. Almost singular inertia tensor may lead to accuracy of 80°. Gaussian inertia moments with means set as nominal ones and with 10% difference for at least one inertia moment normally worsen accuracy only slightly. However some inertia tensors may lead to unacceptable accuracy. For example inertia tensor $\mathbf{J} \approx \mathrm{diag}(5836, 2468, 3600)$ *kg·m²* allows accuracy of 60°. The same goes to inertia tensor $\mathbf{J} \approx \mathrm{diag}(6325, 2491, 4122)$ *kg·m²* if constant and Gaussian disturbances are taken into account. Inertia tensor error itself is not the main source of problems. PD-controller based control is very sensitive to control parameters. So parameters adjusted for some inertia tensor may turn inappropriate for even slightly different one. Fig. 3.7 represent simulation results for inertia $\mathbf{J} \approx \mathrm{diag}(5440, 2241, 3600)$ *kg·m²* with Gaussian disturbance.

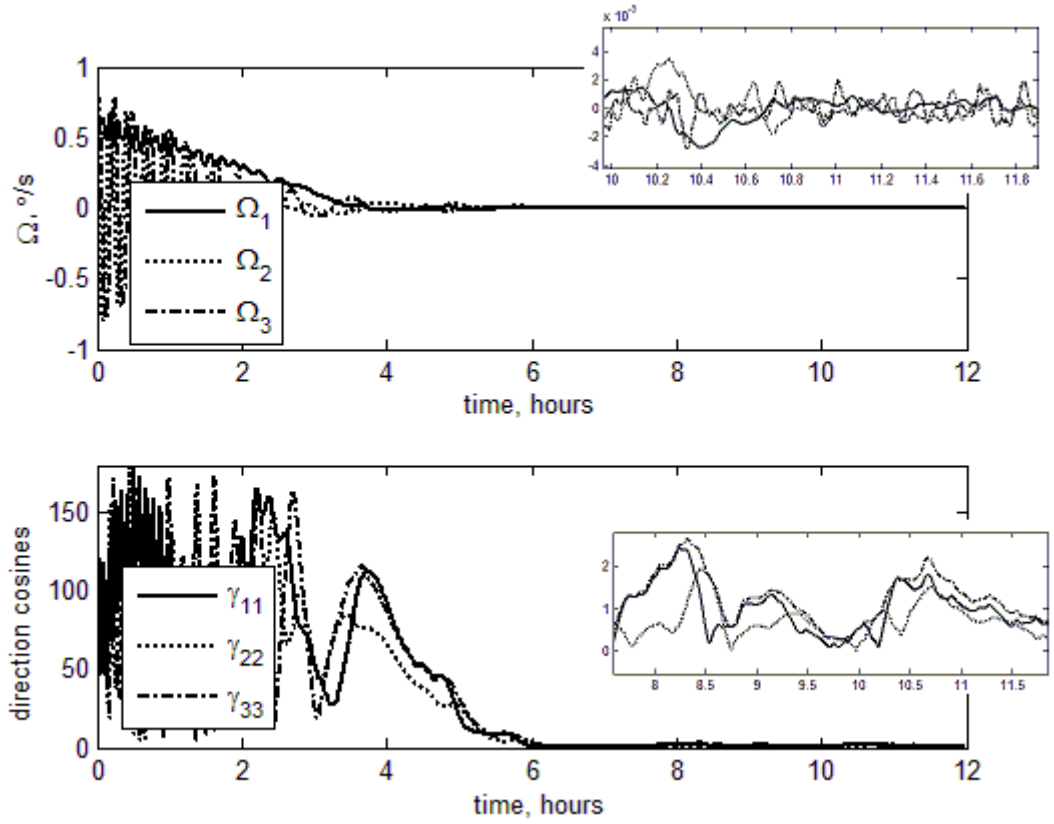

Fig. 3.7. Three-axis attitude, Kalman filter, Gaussian disturbance, inertia tensor error

Accuracy falls to 2.5°. Fig 3.8 presents the same result for constant and Gaussian disturbance.

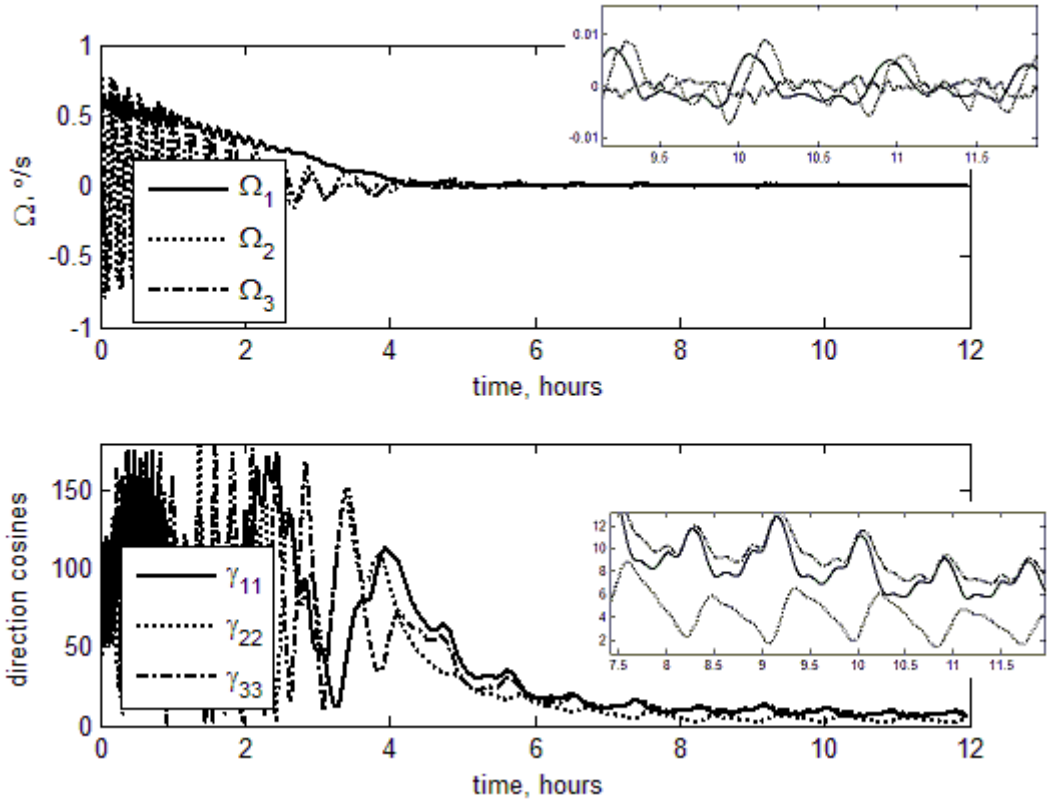

Fig. 3.8. Three-axis attitude, Kalman filter, constant and Gaussian disturbance, inertia tensor error

Accuracy is about 10° for "real" inertia tensor $\mathbf{J} \approx \mathrm{diag}(6325, 2351, 4035)$ *kg·m*^{2}. Maximum constant disturbing torque can easily make the satellite uncontrollable. In most cases however even inertia tensor uncertainty does not severely hampers control algorithm performance.

Conclusion

Fully magnetic control system consisting of magnetorquers and magnetometer is shown to be capable of providing three axis orbital attitude. Accuracy is 1.5-15 degrees depending on disturbing torques acting on the satellite. Accuracy worsens as disturbing torque constant component rises. Inertia tensor uncertainty of 10% level generally leads to accuracy degradation by a factor of 1.5 however uncontrollable motion may occur. Constant disturbing torque due to aerodynamic or solar radiation pressure necessitates inertia tensor and/or control parameters in-flight adjustment.

Bibliography

1. Ovchinnikov M.Y., Roldugin D.S., Penkov V.I. Three-axis active magnetic attitude control asymptotical study // Acta Astronautica. 2015. V. 110. pp. 279–286.
2. Ovchinnikov M.Y. et al. Sliding mode control for three-axis magnetic attitude // Keldysh Institute Preprints. 2014. № 56. 13 p.

3. Abdelrahman M., Park S.-Y. Integrated attitude determination and control system via magnetic measurements and actuation // Acta Astronautica. 2011. V. 69, № 3-4. pp. 168–185.
4. Psiaki M.L., Martel F., Pal P.K. Three-axis attitude determination via Kalman filtering of magnetometer data // J. Guidance Control and Dynamics. 1990. V. 13, № 3. pp. 506–514.
5. Humphreys T.E. et al. Magnetometer-Based Attitude and Rate Estimation for Spacecraft with Wire Booms // J. Guidance Control and Dynamics. 2005. V. 28, № 4. pp. 584–593.
6. Psiaki M.L. Global Magnetometer-Based Spacecraft Attitude and Rate Estimation // J. Guidance Control and Dynamics. 2004. V. 27, № 2. pp. 240–250.
7. Ma H., Xu S. Magnetometer-only attitude and angular velocity filtering estimation for attitude changing spacecraft // Acta Astronautica. 2014. V. 102. pp. 89–102.
8. Searcy J.D., Pernicka H.J. Magnetometer-Only Attitude Determination Using Novel Two-Step Kalman Filter Approach // J. Guidance Control and Dynamics. 2012. V. 35, № 6. pp. 1693–1701.
9. Cote J., Lafontaine J. Magnetic-only orbit and attitude estimation using the square-root unscented Kalman filter: application to the PROBA-2 spacecraft // AIAAGuidance, Navigation and Control Conference and Exhibit, Hawaii, August 2008, pp.1–24.
10. Abdelrahman M., Park S.-Y. Simultaneous spacecraft attitude and orbit estimation using magnetic field vector measurements // Aerospace Science and Technology. 2011. V. 15, № 8. pp. 653–669.
11. Ovchinnikov M., Ivanov D. Approach to study satellite attitude determination algorithms // Acta Astronautica. 2014. V. 98. pp. 133–137.
12. Kalman R.E., Bucy R.S. New Results in Linear Filtering and Prediction Theory // Transactions ASME, Ser. D, J. Basic Engineering. 1961. V. 83. pp. 95–108.
13. Kalman R.E. A New Approach to Linear Filtering and Prediction Problems // Transactions ASME, Ser. D, J. Basic Engineering. 1960. V. 82. pp. 35–45.
14. Wertz J.R. Spacecraft Attitude Determination and Control. Dordrecht/Boston, London: Acad. press, 1990.
15. Belyaev M.Y., Monakhov M.I., Sazonov V.V. Accuracy estimation of the magnetometer measurements onboard Service Module of ISS // Keldysh Institute Preprints. 2012. № 54. 32 p (in Russian).
16. Slotine J.-J., Li W. Applied nonlinear control. Englewood Cliffs: Prentice Hall, 1991. 461 p.
17. Malkin I.G. Some problems in the theory of nonlinear oscillations. Oak Ridge: U.S. Atomic Energy Commission, Technical Information Service, 1959.